Heat recovery from EAF off-gas for steam generation: analytical exergy study of a sample EAF batch

authored by K. Gandt, T. Meier, T. Echterhof, H. Pfeifer

and published in *Ironmaking & Steelmaking*

Contact

Department for Industrial Furnaces and Heat Engineering
RWTH Aachen University
Kopernikusstr. 10
52074 Aachen, Germany

Website: www.iob.rwth-aachen.de/en/
E-mail: contact@iob.rwth-aachen.de
Phone: +49 241 80 25936
Fax: +49 241 80 22289

Heat Recovery from EAF Off-Gas for Steam Generation:

Analytical Exergy Study of a Sample EAF Batch

Karima GANDT, Thomas MEIER, Thomas ECHTERHOF and Herbert PFEIFER

Karima GANDT, gandt@iob.rwth-aachen.de

Thomas MEIER, meier@iob.rwth-aachen.de

Dr.-Ing. Thomas ECHTERHOF, echterhof@iob.rwth-aachen.de → Corresponding author

Prof. Dr.-Ing. Herbert PFEIFER, pfeifer@iob.rwth-aachen.de

RWTH Aachen University

Department of Industrial Furnaces and Heat Engineering

Kopernikusstr. 10

52074 Aachen, Germany

Phone: 0049 - 241 - 25958

Abstract

The high amount of latent and sensible enthalpy discharged from the melting process in an electric arc furnace (EAF) through the off-gas offers high potential for waste heat recovery. Evaporative cooling systems (ECS) installed at dedusting systems of some EAFs are utilising this waste heat for steam generation and subsequent usage of steam for further applications. Within the following paper, further optimisation approaches of this waste heat recovery are examined comparatively by means of exergetic analysis. Thereby, the focus is on the excessive intake of false air into the dedusting system to ensure a complete CO post-combustion. While a sheer energetic examination of the enthalpy hardly shows any differences, the exergetic calculation confirms the significantly higher amount of generated steam with controlled false air ingress. For the calculated optimal reference case with stoichiometric post-combustion, between 50 and 70 % more steam could be produced. Even though a stoichiometric post-combustion cannot be realised for safety reasons, the calculation shows the potential of controlled false air intake for CO post-combustion.

Keywords

electric arc furnace (EAF), evaporative cooling system (ECS), exergetic analysis, off-gas post-combustion, off-gas energy recovery

List of Symbols

Δh_{vap}	specific heat of vaporisation
B	exergy
$\dot{B}$	exergy flow
c_p	specific heat capacity
$\dot{H}$	enthalpy flow
h	specific enthalpy
m	mass
$\dot{m}$	mass flow
$\dot{n}$	amount of substance flow
p	pressure
R	universal gas constant
s	specific entropy
T	temperature
t	time
$\dot{V}$	volume flow
x	amount-of-substance fraction
η	efficiency factor
ρ	density

List of Subscripts and Superscripts

"	vapour line
$\cdot$	flow
I	case of stoichiometric combustion calculation

II	case of overstoichiometric combustion calculation
a	ambient
abs	absolute
ch	chemical
CS	cooling steam
FA	false air
FG	flue gas
hv	heating value
max	maximum
mix	mixture of gases
i	substance i
OG	off-gas
SATP	standard ambient temperature and pressure
STP	standard temperature and pressure
th	thermal
tot	total
transf	transferred
vap	vaporisation
W	water

1. Introduction

Electric steelmaking in an electric arc furnace (EAF) is the second most important steel production route and the most significant one for scrap recycling. Although the process is already highly optimised, in times of sustainability and resource conservation it is still necessary to consider further optimisation potentials to enhance efficiency. The mostly unused waste heat of the EAF off-gas worsens the efficiency of the process enormously. Up to 50 % of all energy losses[1)] and about 30 % of the total energy input are wasted with the flue gas from the process.[2-4)]

In order to avoid uncontrolled dust, CO and H_2 emissions, the off-gas has to be exhausted from the EAF. All combustible substances must be completely post combusted. Since high temperatures of up to 2,000 K are occurring in current exhaust system, the flue gas (for a better distinction the post-combusted EAF off-gas is referred to as flue gas) must be cooled down before the filtering.

A simple approach for recovering energy from the flue gas is the generation of steam, which is further used in the steelworks. Here, the cooling medium is water in boiling state which evaporates during the cooling process. The steam is generated while the latent part of the off-gas energy is converted to sensible heat. Due to the second law of thermodynamics, these energy conversions and heat transfers cannot take place arbitrarily and not without any dissipation. Therefore, the quality of the energy transfer from the EAF off-gas to the flue gas and afterwards to the steam is analysed and evaluated with an exergy analysis and assessment. Energy consists of exergy, the part of the energy which can be converted into any other form of energy, and anergy, the remaining part of the energy, that cannot be applied for mechanical work. Exergy can be converted to anergy, but not vice versa. The aims of the calculations are to achieve an optimal and most efficient way of heat recovery and to identify potentials for optimisation. The most efficient heat recovery system transfers highest ratios of the off-gas exergy into the steam with low exergy losses.

In this work, the exergy transfers are calculated by way of example. Therefore, the process steps when anergy arises can be recognised in principle. Weak points of the heat transfer in an EAF waste heat process can be identified and strategies for solutions can be found.

The basis for the analysis within this paper is the data of a sample batch of a sample EAF. First, the exergy of the furnace off-gas (indexed in formulae with OG) is determined. Then, the exergy losses, caused by the post-combustion of the off-gas' H_2 and CO with false air (indexed with FA), and thus the flue gas (indexed with FG) exergy flow are calculated. Subsequently, an ideal heat transfer between the flue gas and the boiling water is assumed and for typical input data of ECSs the exergy of the cooling steam (indexed with CS) is determined. The calculation results are available for eight different cases, which are compared at the end. Finally, optimisation potentials for an efficient heat recovery from EAF off-gases are shown.

2. State of the Art

State of the art technique is a water pipe cooling and/or air or water quenches in the very first beginning of the dedusting system as a minimum standard. The cooling water's input properties are usually standard ambient temperature and pressure (SATP) and the absorbed heat is not utilised.

The idea of evaporative cooling instead of ordinary water cooling is long-established. With the development of ultra-high-power-EAFs in the seventies and eighties, an improved cooling was necessary. In addition to simple cold water cooling, the advantage of increasingly warm and hot water cooling was taken into consideration, leading to an increased use of evaporative cooling systems (ECS). Some ECSs have been successfully used in industrial EAFs[4,5] and this technique is state-of-the-art in basic oxygen furnace processes.[3] Current industrial ECSs (depending on EAF operation, off-gas volume flow and temperature) are generating 0.15 to 0.225 tons of steam per ton of steel.[4,5] However, since an ECS operates at a higher pressure level, the conventional cooling pipes must be replaced by pressure-resistant ones. These

additional investment costs are mostly the reason why old EAFs are not modified yet. Only newly-built furnaces, which are designed for highest efficiency, are often directly provided with an ECS.[5)]

One important advantage of the evaporative cooling is the high heat adsorption capacity. Heat can be sensibly or latently stored in a cooling medium. Sensible means, that the temperature of the cooling medium increases with the input of energy. If the coolant changes its phase, within an ECS from liquid to gaseous, the heat is latently stored and used for evaporation and the temperature does not increase as a consequence. The enthalpy of vaporisation of water is higher than the heat adsorption capacity of liquid water. This means, that in contrast to sensible cooling with less cooling mass more heat can be extracted from the EAF flue gas. In an ECS, it must be ensured that the water is only partially vaporised, as the heat transfer to superheated steam is low and a safe cooling would no longer be guaranteed.

If the generated steam is further utilised in the plant system, the efficiency of the EAF process will increase. There are several opportunities of using steam in the steel plant, e.g. vacuum degassing, generation of electricity, generation of oxygen or air conditioning. It is essential to design the ECS regarding the different requirements of the steam applications concerning steam mass, temperature and pressure.

3. Calculations

3.1 Assumptions

The exergy potential of the off-gas and the resulting steam is calculated on the basis of a sample batch. This is feasible, because the EAF process is sufficiently similar in different steelworks. Temperatures and flow rates are never identical but in a sufficiently similar magnitude. Furthermore, the process steps of the exergy losses and their relative magnitude, not absolute, are of interest.

The average European EAF has a 2 or 3-basket strategy [6-8)] and characteristics listed in **Table 1**. To be able to determine the holistic exergy transfer from the EAF off-gas to the coolant,

extensive data of a batch (temperature, volume flow and composition from the off-gas at every point of time) is required. Valuated data is provided by measurements accomplished by the Department of Industrial Furnaces and Heat Engineering of the RWTH Aachen University.[9] The corresponding properties of the EAF, where the measurements were performed, are listed in **Table 2**.

The analytical exergy study includes the following calculation sub-steps:

1. off-gas exergy flow with the data of the sample EAF,
2. flue gas temperature or adiabatic combustion temperature, respectively,
3. heat transfer from the flue gas to the coolant,
4. resulting steam mass flow,
5. steam exergy flow,
6. efficiency.

The following assumptions are made:

- ambient temperature T_a = 300 K
- ambient pressure p_a = 0.1 MPa
- reference point for balances: T_a and p_a
- no pressure losses
- elements of off-gas: N_2, O_2, CO, CO_2, H_2, H_2O
- elements of flue gas: N_2, O_2, CO_2, H_2O
- molar composition of false air: $x_{FA,N2}$ = 0.79 and $x_{FA,O2}$ = 0.21
- Heat capacities of all gases are calculated with the NASA polynomials.[10]

$$c_p(T) = R\left(A + BT + CT^2 + DT^3 + ET^4\right) \quad (1)$$

where R represents the universal gas constant (R = 8.315 J mol^{-1} K^{-1}), and A to E are the substance-specific NASA-polynomial-constants.[10]

The averaged heat capacity in a wide temperature range (from T_1 to T_2) is[11]

$$c_p\Big|_{T_1}^{T_2} = \frac{\int_{T_1}^{T_2} c_p(T)\,dT}{T_2 - T_1} \tag{2}$$

- The heat capacity of a mixture of gases is[11,12)]

$$c_{p,mix}(T) = \sum x_i \; c_{p,i}(T) \tag{3}$$

- Other material data (e.g. mol masses, properties of water at saturation condition) is taken from [11-13)].

3.2 Calculations of the Off-Gas Exergy Flow

Fig. 1 (a) and **(b)** are showing the most important off-gas properties like the temperature T_{OG}, the normal volume flow rate $\dot{V}_{STP,OG}$ and the molar composition $x_{OG,i}$ of the sample batch are shown. The elements N_2 and H_2O are not displayed since N_2 is inert and the molar proportion of H_2O in the off-gas is less than 3 mol-% and therefore neglected.

The total exergy flow of the EAF off-gas $\dot{B}_{OG}$ consists of a thermal ($\dot{B}_{OG,th}$) and a chemical part ($\dot{B}_{OG,ch}$). The thermal exergy is characterised by the temperature difference between off-gas and reference point, while the chemical exergy has its origin in not completely combusted off-gas compounds like CO and H_2. There are other forms of exergy (e.g. potential or kinetic exergy), which are neglected in this calculation, because their amount is vanishingly low. Thus, the total exergy flow of the EAF off-gas $\dot{B}_{OG}$ is calculated according the **Equation (4)**, **(5)** and (**6).**[11,12)]

$$\dot{B}_{OG} = \dot{B}_{OG,th} + \dot{B}_{OG,ch} \tag{4}$$

with

$$\begin{aligned} \dot{B}_{OG,th} &= \dot{n}_{OG} \sum x_{OG,i} \left[\Delta h_i(T) - T_a\, \Delta s_i(T)\right] \\ &= \dot{n}_{OG} \sum x_{OG,i} \left[\int_{T_a}^{T_{OG}} c_{p,OG,i}(T)\,dT - T_a \int_{T_a}^{T_{OG}} \frac{c_{p,OG,i}(T)}{T}\,dT\right] \end{aligned} \tag{5}$$

and

$$\dot{B}_{OG,ch} = \dot{n}_{OG,CO}\left[\Delta H^{o}_{c,CO}(T_a) + T_a\ (s_{CO2,abs} - s_{CO,abs} - 0.5\, s_{O_2,abs})\right] + \dot{n}_{OG,H_2}\left[\Delta H^{o}_{c,H_2}(T_a) + T_a\,(s_{H_2O,abs} - s_{H_2,abs} - 0.5\, s_{O_2,abs})\right] \quad (6)$$

3.3 Calculations of the Flue Gas Temperature and Exergy Flow

The first exergy loss is caused by the mixing of the off-gas with the false air. Thermal exergy is transformed into anergy, since the false air reduces the off-gas temperature level. This is of particular relevance with excessive false air ingress.

The first exergy loss is caused by the post-combustion. The flue gas temperature T_{FG} is the adiabatic combustion temperature and is calculated for complete post-combustion of CO and H_2. The expectation of an adiabatic reaction does not reflect reality, since the off-gas is already cooled during the post-combustion by the ECS, but this is the easiest and only way to show the exergy loss due to the conversion of chemical to thermal exergy. The main amount of the required false air is drawn at the annular gap behind the elbow and has ambient temperature. Two combustion cases are calculated: First, the false air input is assumed to be controlled in a way that a stoichiometric combustion is realised (indexed with I). This represents an ideal optimised process. For the second combustion case, an overstoichiometric combustion with a four times greater air ingress through the annular gap is calculated (indexed with II). This represents roughly the current industrial EAF process.

As described above, the flue gas temperature level of adiabatic combustion cannot be achieved in reality. To calculate the flue gas temperature T_{FG}, the enthalpy flow balance, consisting of flue gas ($\dot{H}_{FG}$), off-gas ($\dot{H}_{OG}$) and false air ($\dot{H}_{FA}$) thermal enthalpy and the chemical off-gas enthalpy, represented by the heating value $\dot{H}_{hv,OG}$, is solved iteratively via **Equation (7)**, **(8)** and **(9)**.

$$\dot{H}_{FG}(T_{FG}) = \dot{H}_{OG}(T_{OG}) + \dot{H}_{FA}(T_a) + \dot{H}_{hv,OG}(T_a) \quad (7)$$

with

$$\dot{H}_{OG}(T_{OG}) = \dot{n}_{OG} \int_{T_a}^{T_{OG}} c_{p,OG}(T_{OG})\, dT$$
$$\dot{H}_{FA}(T_a) = 0$$
$$\dot{H}_{hv,OG}(T_a) = \dot{n}_{OG,CO}\, H_{hv,CO}(T_a) + \dot{n}_{OG,H_2}\, H_{hv,H_2}(T_a) \quad (8)$$
$$\dot{H}_{FG}(T_{FG}) = \dot{n}_{FG} \int_{T_a}^{T_{FG}} c_{p,FG}(T_{FG})\, dT$$

$$T_{FG} = \frac{\dot{H}_{OG}(T_{OG}) + \dot{H}_{hv,OG}(T_a)}{\dot{n}_{FG} \int_{T_a}^{T_{RG}} c_{p,FG}(T_{FG})\, dT} + T_a \quad (9)$$

With the post-combustion, the chemical exergy is transformed into anergy and thermal exergy. In comparison to the off-gas, the flue gas has a lower thermal exergy and no more chemical exergy. The exergy flow is calculated according to Equation 4, indexed with FG for the flue gas instead of OG for the off-gas.

3.4 Calculations of the Steam Coolant Mass Flow and Exergy Flow

The relevant heat transfer mechanisms from the gas to the cooling medium are convection, conduction and radiation. Apart from the temperature difference of the two fluids, many values, e.g. fluid substance properties (dependent on temperature), mass flow, composition, dust loading and geometric data of the dedusting system have to be known or to be assumed. It is necessary to avoid that the calculation of the heat transfer takes effect on the exergy calculation because the comparability of the two combustion cases would no longer be feasible. In order to maintain this comparability, only an ideal heat transfer is considered. For this purpose, the pinch point method is used.

The pinch point method is a method to design a heat exchanger according to a minimum predetermined temperature difference.[11)] In this calculation, the temperature difference is the one between the flue gas and the coolant water at boiling point and is set to an assumed value of 100 K. The assumption of a constant temperature difference and a constant coolant temperature simplifies the calculation, as an overheating of the steam is excluded and thus the

steam temperature is non-varying in the wet steam region. In principle, the temperature difference can be chosen variously and differs from reality, which is a weakness of the calculation.

Furthermore, a controlled water flow through the cooling pipe is assumed so that no heat transfer from the cooling media to the flue gas can occur in times where the flue gas temperature is below the boiling temperature. The molar flow of necessary coolant $\dot{n}_{CS}$ is calculated with the enthalpy balance according to **Equation (10)** and (**11)**. Since the non-vaporised water remains in the cooling circuit and does not absorb any energy, it does not have to be observed in the enthalpy balance.

$$\dot{H}_{FG}(T_{FG}) = \dot{H}_{CS}(T_{CS}) \tag{10}$$

$$\forall\ T_{FG} > T_{CS}:\ \dot{n}_{CS} = \frac{\dot{n}_{FG} \int_{T_{CS}+100\,K}^{T_{FG}} c_{p,FG}(T)\,dT}{\Delta h_{vap}} \tag{11}$$

$$\forall\ T_{FG} \leq T_{CS}:\ \dot{n}_{CS} = 0\,\mathrm{mol\,s^{-1}}$$

Usual ECSs are operated with water/steam pressures of 1 to 4 MPa. Four pressure cases are further investigated: 1 MPa, 2 MPa, 3 MPa and 4 MPa. Thus, the input temperatures of the boiling water are the corresponding boiling temperatures to be looked up in steam tables as well as the heats of vaporisation Δh_{vap}.[11-13)]

The steam contains only thermal exergy. With the data of steam at vapour line conditions (indexed with ″), the steam exergy flow $\dot{B}_{CS}$ is computed via **Equation (12)**. The knowledge of the steam exergy and its mass flow or total mass is important for the estimation of possible applications.

$$\dot{B}_{CS} = \dot{n}_{CS}\,[(h'' - h_a) - T_a\,(s'' - s_a)] \tag{12}$$

The exergy flow of the input boiling water $\dot{B}_W$ is calculated with **Equation (13)**. This is necessary to obtain information about the necessary input of energy for the pressurisation and heating of the cooling water before its usage in the ECS. In addition to the entire steam exergy

flow $\dot{B}_{CS}$, the transferred one from the flue gas to the steam ($\dot{B}_{trans,FG\text{-}CS}$) is of interest. The result of the difference between the steam exergy $\dot{B}_{CS}$ and the water exergy $\dot{B}_W$ leads to the transferred exergy amount in **Equation (14)**.

$$\dot{B}_W = \dot{n}_W [\Delta h - T_a \Delta s] \quad (13)$$

with

$$\dot{n}_W = \dot{n}_{CS}$$
$$\Delta h = h(p) - h_a$$
$$\Delta s = s(p) - s_a$$

$$\dot{B}_{trans,FG-CS} = \dot{B}_{CS} - \dot{B}_W \quad (14)$$

3.5 Calculations of the Heat Transfer Efficiency

In order to evaluate the steam generation, it is suitable to determine the efficiency η of the entire heat recovery process (including mixing, post-combustion, pressurising and heating). Thus, the final steam exergy is related to the initial exergy value via **Equation (15)**.

$$\eta = \frac{\dot{B}_{CS}}{\dot{B}_{OG} + 1.3\,\dot{B}_W} \quad (15)$$

The factor 1.3 means, that the preparation of the water (pressurisation and heating) is operated with losses. The percentage proportion is usually in the range from 10 to 40 % and is assumed and set to 30 %.[14)]

4. Results and Discussion

4.1 Calculations concerning the Off-Gas

The amount of exergy leaving the sample EAF is identified at the beginning of the whole calculation. From the available data it is determined, that the total off-gas exergy of the sample batch is B_{OG} = 45 GJ per batch, leading to an average exergy flow of $\dot{B}_{OG}$ = 9.4 MW, respectively. The chemical exergy content is approximately 65 %, the sensible part caused by the temperature level accordingly 35 %.

4.2 Calculations concerning the Flue Gas

Due to the mixing of the off-gas with false air and the following post-combustion, part of the exergy is transformed into anergy. The mixing ratio of off-gas and false air defines the off-gas false air mixture temperature $T_{mix,OG\text{-}FA.}$ Its level is below the off-gas temperature T_{OG} and is dependent on the mixing ratio, thus whether combustion case I or II is present. The flue gas temperature level as endpoint for post-combustion interdepends on the post-combustion starting temperature, which is the off-gas false air mixture temperature $T_{mix,OG\text{-}FA.}$ The temperatures $T_{mix,OG\text{-}FA}$ and T_{FG} are printed in **Fig. 2** for both combustion cases. As can be seen, the temperature level for the real process (combustion case II) is significantly below the one with stoichiometric post-combustion (combustion case I). The maximum flue gas temperature levels are $T_{max,FG,I}$ = 3,060 K and $T_{max,FG,II}$ = 1,599 K, respectively.

Particularly in the second combustion case, the mixing with false air converted an important amount of exergy to anergy. The total flue gas exergy of the stoichiometric calculation case is $B_{FG,I}$ = 42 GJ per batch, which is equivalent to an average exergy flow of $\dot{B}_{FG,I}$ = 8.7 MW. The total flue gas exergy of the overstoichiometric calculation case amounts to $B_{FG,II}$ = 27 GJ per batch, corresponding to an average exergy flow of $\dot{B}_{FG,II}$ = 5.6 MW, respectively. Because of the mixture and post-combustion 7.4 % (combustion case I) and 40.2 % (combustion case II) of exergy are converted to anergy. At this point it is already obvious, that less steam is generated in the second case compared to the first combustion case.

The two combustion cases differ especially in the different mass flow rates of the flue gas. The result is, that the thermal enthalpies are effectively identic ($H_{FG,I} \approx H_{FG,II} \approx$ 57,100 GJ per batch), but the exergy flows are different due to the temperature level differences. Under real conditions, the lower temperature level in the second combustion case leads to a lower heat transfer.

For optimisation of the post-combustion in the dedusting system, the chemical reaction has to be ensured first. However, a stoichiometric one is not realisable, but a controlled post-combustion is entirely feasible. The secondary air control is currently a research topic. There

are few concepts that contribute this process optimisation, although there are reliable real-time off-gas analysis systems, which are currently used for the control of the oxygen lances only (e.g. the systems LINDARC® from Linde Group or EFSOP® from Tenova Goodfellow).

In addition, it is possible to control the location of the post-combustion. It has to be considered, whether a post-combustion in the furnace vessel or in the exhaust pipe is more efficient. It might be more economic to release the combustion energy in the cooling system and thus to generate more steam. During the flat bath at the end of the melting process in an EAF, the liquid melt is covered with slag. Therefore, the heat of post-combustion would not be sufficiently transferred from the furnace atmosphere to the melt, since the heat energy is primarily transmitted by radiation. The necessary considerations are possible by using process models and process simulations.[15)]

4.3 Calculations concerning the Steam Coolant

With the flue gas temperature, the total masses and the exergy flow of the generated steam are calculated for four different water pressure levels (1 MPa, 2 MPa, 3 MPa and 4 MPa). The results are given in **Table 3**.

The total mass of steam generated in the second combustion case is almost constant ($m_{CS,tot,II}$ = 16.1…16.5 t), since steam is only produced if the flue gas temperature is lower than the boiling temperature of the water. This mostly applies to the second calculation combustion case, where the time sections with no steam production are getting larger. In the first combustion case, the increase of the total steam mass ($m_{CS,tot,I}$ = 25.3…28.8 t) with increasing pressure level is self-evident, as Δh_{vap} decreases and more cooling medium is necessary to adsorb the same amount of heat.

Since the total exergy of the steam is directly dependent on the generated steam mass flow, the total amount of exergy in the first combustion case increases ($\dot{B}_{CS,I}$ = 4.3…4.9 MW or $B_{CS,I}$ = 20…23 GJ) but remains nearly constant in the second combustion case ($\dot{B}_{CS,II}$ = 2.8…2.7 MW or $B_{CS,II}$ = 13 GJ) for the varying pressures.

Although higher pressure means a higher exergy level, the investment costs increase with increasing pressure level, because the system components have to be designed more robust. An additional consideration is that the steam must be prepared according to the pressure and temperature level at its boiling point. The higher the level, the more energy has to be spent on heating and pressurising before. For the first combustion case, an amount of $\dot{B}_{W,I}$ = 0.7…1.5 MW is needed, in the second one $\dot{B}_{W,II}$ = 0.4…0.9 MW.

The proportion of exergy that can be transferred from the flue gas to the steam decreases from 41.4 to 39.1 % in the first combustion case and 42.9 to 32.0 % in the second one. The reason is, that the flue gas can be cooled less due to the increasing steam temperatures.

An analysis of the theoretical limits of the heat transfer process shows, that there is an upper limit: the critical point of water (647.25 K and 22.12 MPa). Until this upper limit the transferable exergy from the flue gas to the steam decreases, but the generated steam mass and steam exergy increase.

4.4 Efficiency of the Heat Transfer Process

The final calculation step is the determination of the efficiencies η_I and η_{II} of the heat recovery processes, which are also listed in Table 3. As can be seen, the efficiencies η_I and η_{II} are almost constant for all pressure cases. η_I is in the range from 0.42 to 0.43 and η_{II} from 0.28 to 0.26.

A comparison of the two 4 MPa pressure cases shows the influence of the amount of false air ingress and the importance of a controlled false air input. **Fig. 3 (a)** and **(b)** consists of two Sankey diagrams, which are illustrating the exergy flows and the itemised steps of exergy flow losses.

The steam exergy level in the second combustion case is lower than the one in the first combustion case. Nevertheless, the steam is still useful for some applications, for which the temperature and not the exergy is more important. This includes the possibility of building heating among others. For the generation of electricity, the steam is less suitable. Depending

on the available EAF and the individual usability of the steam in the steelwork, it has to be decided precisely which combustion and pressure cases are suitable.

5. Conclusion

Since the steel production in electric arc furnaces (EAF) is the second most important route, the process is already highly optimised. Nevertheless, in the period of economic competition and increasing environmental regulations, other optimisation potentials have to be investigated. One of these potentials is the usually non-used waste heat of the cooling water in the dedusting system. A practical waste heat utilisation within the steel plant is the generation of steam in the cooling pipes by using boiling water as cooling medium. This kind of cooling system is called evaporative cooling system (ECS).

In this publication, the exergy transfer from the EAF off-gas to the generated cooling steam, under the consideration of losses by mixing with false air and post-combustion, is calculated. Therefore, the measured data of a sample batch of a 145 t-EAF is used. As calculation starting point, the exergy of the EAF off-gas of a sample batch is determined to B_{OG} = 45 GJ. Here, the chemical potential of 65 % of this exergy is apparent. The post-combustion and the exergy of the flue gas is then determined. To point out the influence of a regulated false air input, two post-combustion cases are distinguished: On the one hand, a stoichiometric one by an optimal assumed false air control and on the other hand, an overstoichiometric reaction by an air input with a ratio of off-gas to false air flow rate of 1:4. It is shown, that controlled false air ingress leads to higher flue gas exergy ($B_{FG,I}$ = 42 GJ instead of $B_{FG,II}$ = 27 GJ). As a result, a higher exergy transfer to the cooling steam per batch and therefore a higher steam mass is generated.

After the flue gas exergy determination, four different ECS designs are considered. The distinguishing feature is the pressure of the boiling water, which is set to 1, 2, 3 or 4 MPa. Finally, an ideal heat transfer from the flue gas to the coolant and a regulated water flow, which means that no heat transfer from the water to the flue gas can occur, is assumed. The resulting total steam mass and the corresponding total exergy of the steam are determined. In

the first combustion case a total amount of steam $m_{CS,tot,I}$ = 25.3 to 28.8 t with a total exergy $B_{CS,tot,I}$ = 20 to 23 GJ could be produced. However, the efficiency η_I is almost constant for all pressure cases and is in the range from 0.42 to 0.43. Since there are limited numbers of usability, a large steam mass is not necessarily an advantage. Furthermore, with an increased water mass flow rate, the investment costs for a larger cooling system (larger pipes, steam drum, secondary equipment etc.) are higher. Moreover, the effort to set the water of ambient conditions to input temperature and pressure is accordingly higher.

Since the flue gas has already a lower level of exergy in the second combustion case, even less exergy is transferred to the steam ($B_{CS,tot,II}$ = 13 GJ). Due to the regulation of water and lower flue gas temperature, all four pressure cases produce nearly the same total mass of steam ($m_{CS,tot,II}$ = 16.1…16.5 t). In the second case, no high steam exergy level can be achieved. Nevertheless, there are applications, for which the steam temperature and not the exergy is more essential. This applies for example for building heating, but not for the generation of electricity. The required steam parameters in the steelwork and the EAF determine the suitable combustion and pressure cases.

6. References

1. A.-P. Hollands, K. Libera, T. Rummler, R. Hagemann, M. Harde, D. Laing and W.-D. Steinmann: ‘Concepts for energy recovery in mini-mills’, *Stahl Eisen*, 2011, **131** (11), S111-S120.
2. F. Zauner, A. Hampel, G. Enickel, A. Fleischanderl, T. Steinparzer and M. Haider: ‘New developments in efficient energy recovery from electric arc furnace offgas by using innovative themal energy storage systems’, *10th Eur. Electr. Steelmaking Cong., EEC*, Graz, Austria, 25.-28.09.2012, Leoben, Austria, ASMET, 320-329.
3. C. Fröhling, P. Hemmling, J. Kempken and W. H. Emling: ‘How to make the plants of today comply with the requirements of tomorrow’, *Proc. of Iron Steel Technol. Conf. Exhibition, AISTech*, Atlanta, GA, USA, 07.-10.05.2012, Warrendale, PA, USA, AIST, 81-86.
4. C. Born and R. Granderath: ‘Benchmark for heat recovery from the offgas duct of electric arc furnaces’, *MPT* 2013, **36** (1), 32-35.
5. T. Sagermann: 'Weltweit neues Umweltkonzept für Edelstahlherstellung in China', *press release*, (ed. SMS Siemag AG), dated 08.04.2014.
6. Y. N. Toulouevski and I. Y. Zinurov: 'Innovation in electric arc furnaces. Scientific basis for selection', 2010, Heidelberg, Germany, Springer.
7. R. Remus, M. A. A. Monsonet, S. Roudier and L. D. Sancho: 'Best available techniques (BAT) reference document for iron and steel production', EUR25521EN, (ed. Joint Research Centre of the European Commission), 2013, Luxembourg, Publications Office of the European Union.
8. M. Schubert, F. Treptow and K. Timm: 'Lichtbogenöfen', in 'Praxishandbuch Thermoprozesstechnik, Band II: Prozesse, Komponenten, Sicherheit', (eds. A. von Starck, A. Mühlbauer, C. Kramer), 2nd edn, chap. 2.1, 27-53, 2003, Essen, Germany, Vulkan.

9. V. Velikorodov: ‘Der Einfluss der Entstaubung auf den spezifischen elektrischen Energieeinsatz des Lichtbogenofens', PhD thesis, RWTH Aachen University, Aachen, Germany, 2009.
10. B. J. Mcbride, S. Gordon and M. A. Reno: ‘Coefficients for calculating thermodynamic and transport properties of individual species’, *NASA Technical Memorandum 4513*, Washington, D.C., USA, 1993.
11. G. Cerbe and G. Wilhelms: ‘Technische Thermodynamik’, 2008, Munich, Germany, Hanser.
12. K. Lucas: ‘Thermodynamik’, 5th edn, 2006, Berlin, Germany, Springer.
13. Verein Deutscher Ingenieure (ed.): ‘VDI-Waermeatlas’, 10th edn, 2006, Berlin, Germany, Springer.
14. J. F. Gülich: 'Kreiselpumpen', 4th edn, 2013, Berlin, Germany, Springer.
15. T. Meier, A. H. Kolagar, T. Echterhof, H. Pfeifer: “Gas phase modeling and simulation in an electric arc furnace process model for detailed off-gas calculations in the dedusting system”, *STEELSIM 2015*, Bardolino, Italy, 23.-25.09.2015.

List of Captions

Fig. 1. Characteristics of the sample batch.[9)]

(a) Off-gas temperature T_{OG} and off-gas normal volume flow $\dot{V}_{STP,OG}$.

(b) Off-gas composition $x_{OG,i}$.

Fig. 2. Flue gas temperatures T_{FG} in comparison to mixture temperatures $T_{mix,OG\text{-}FA}$.

Fig. 3. Sankey diagrams.

(a) Case of stoichiometric combustion (I).

(b) Case of overstoichiometric combustion (II).

Table 1. Technical parameters of EAFs within the EU.[7)]

Table 2.Technical parameters of the sample EAF.[9)]

Table 3. Results concerning calculations of the steam coolant.

Figures

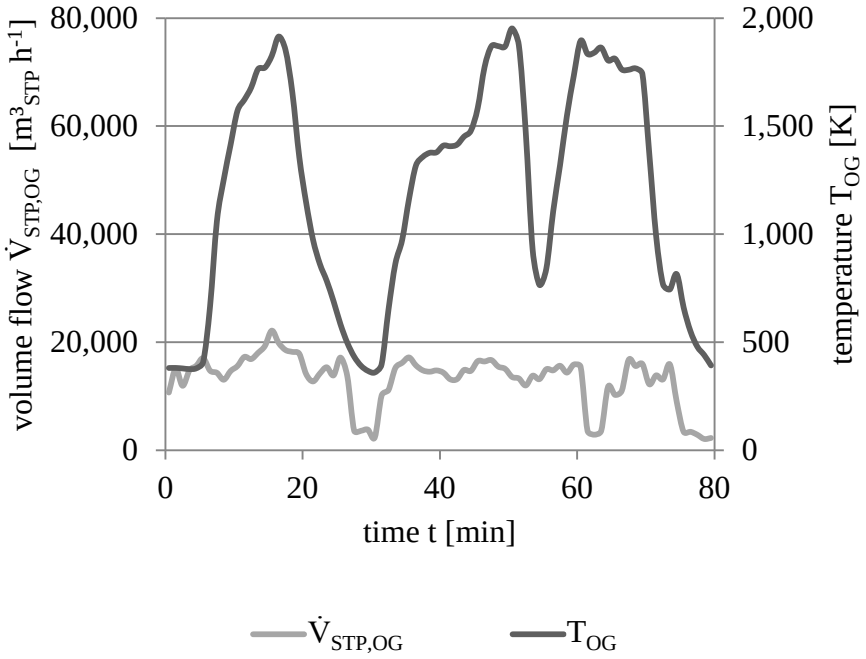

(a) Off-gas temperature T_{OG} and off-gas normal volume flow $\dot{V}_{STP,OG}$.

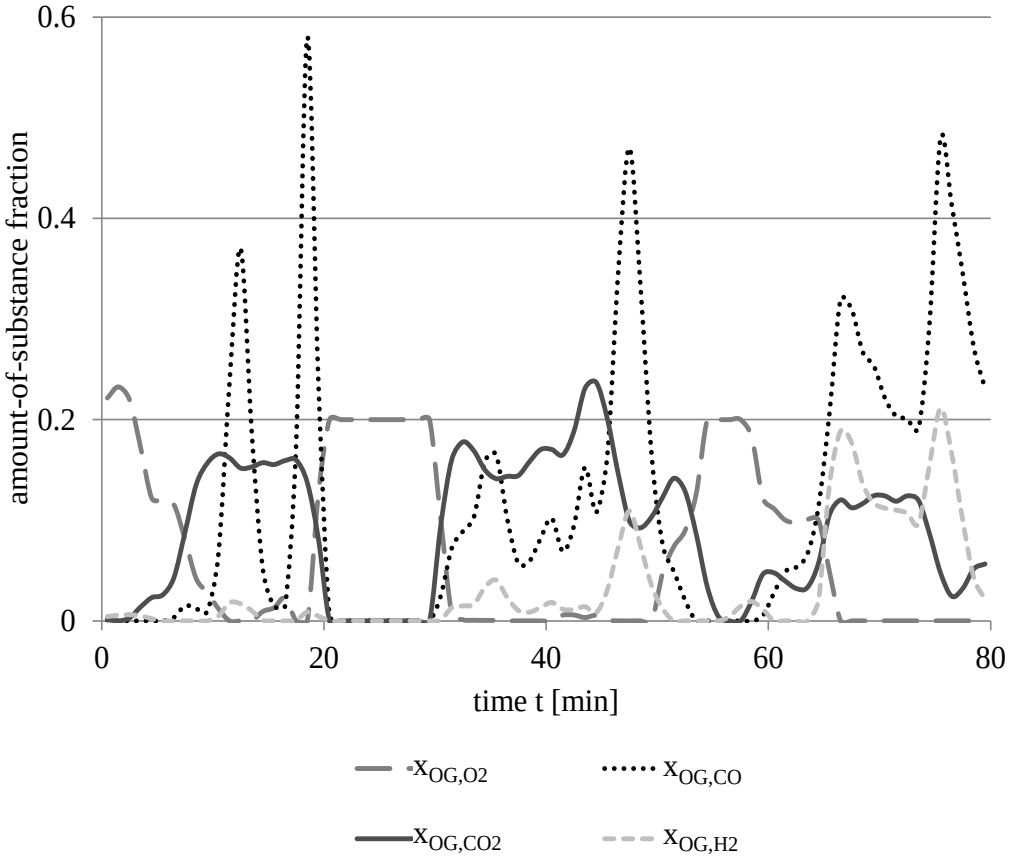

(b) Off-gas composition $x_{OG,i}$.

Fig. 1. Characteristics of the sample batch.[9)]

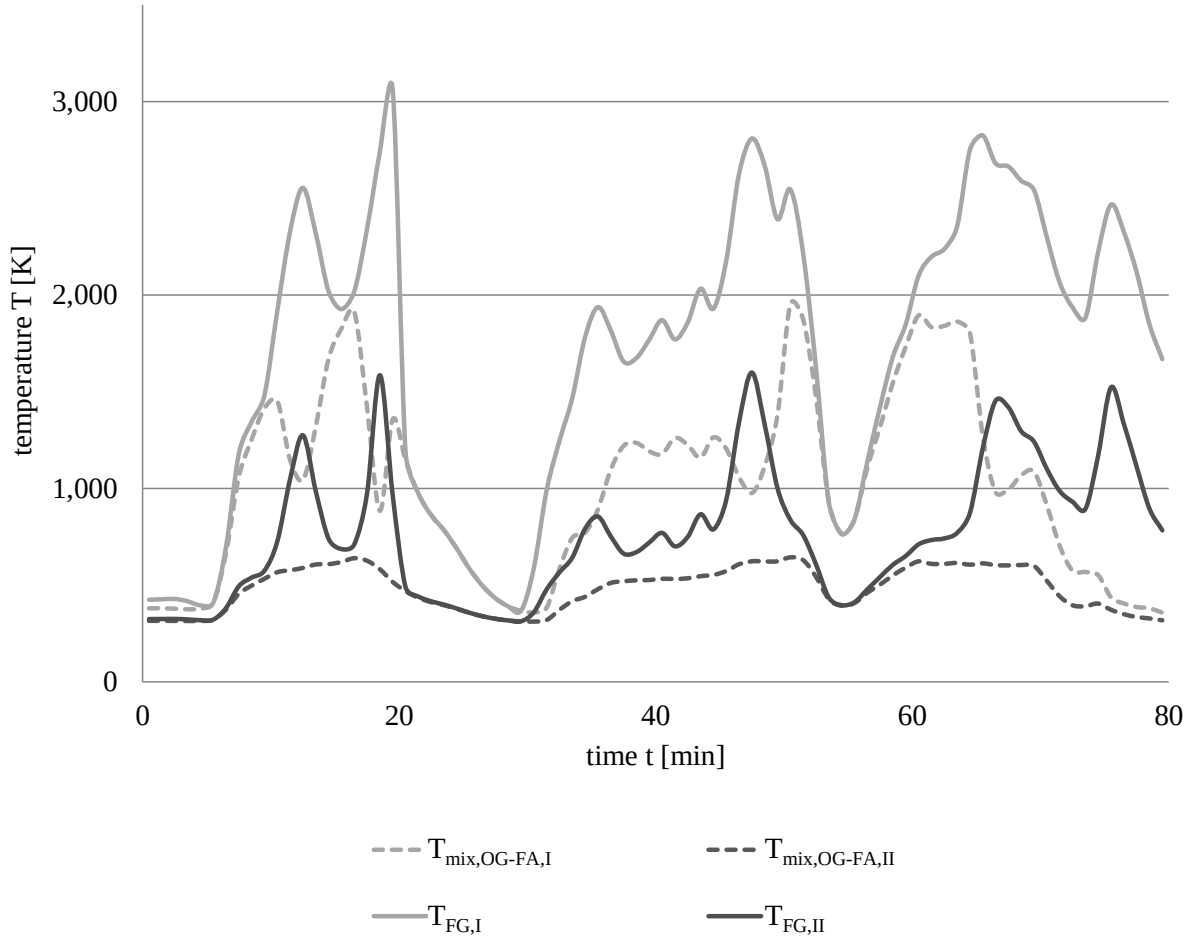

Fig. 2. Flue gas temperatures T_{FG} in comparison to mixture temperatures $T_{mix,OG\text{-}FA}$.

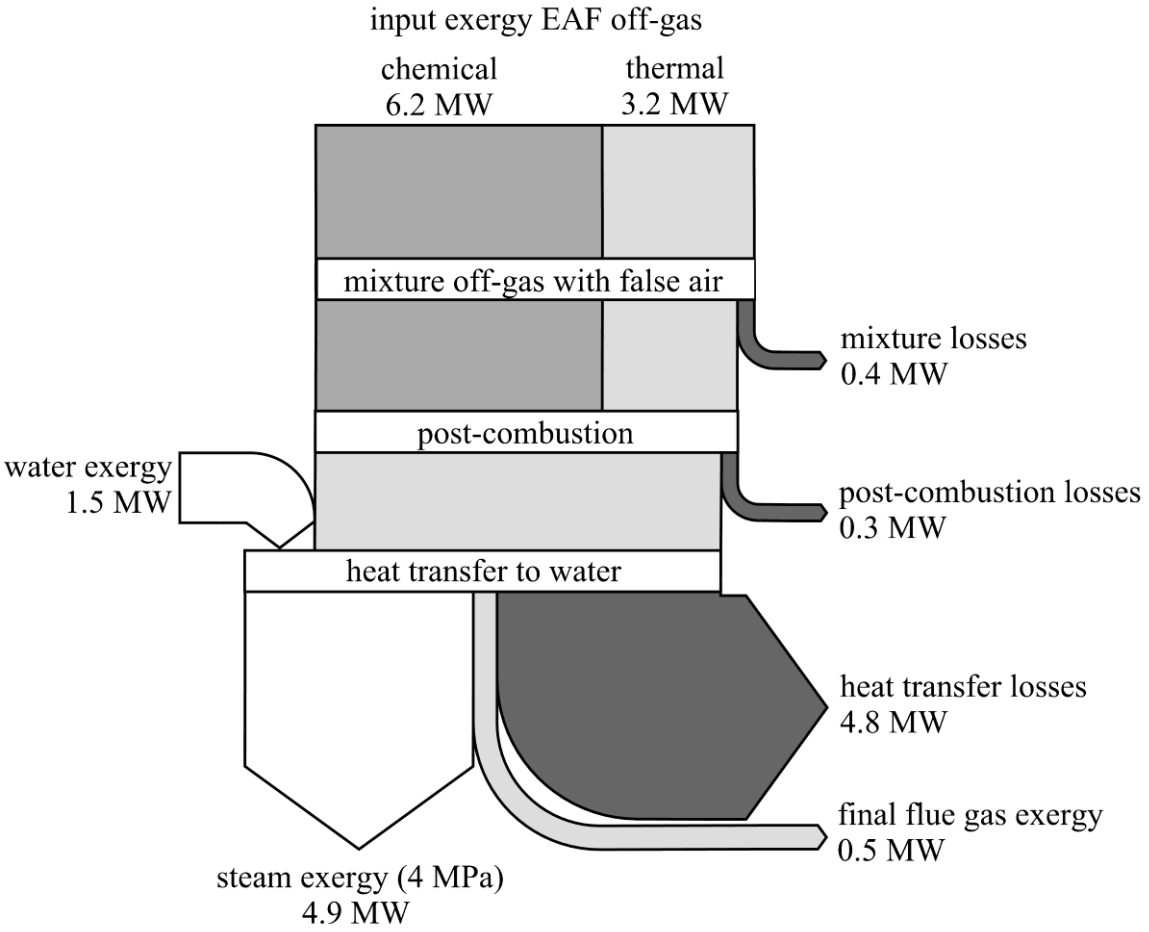

(a) Case of stoichiometric combustion (I).

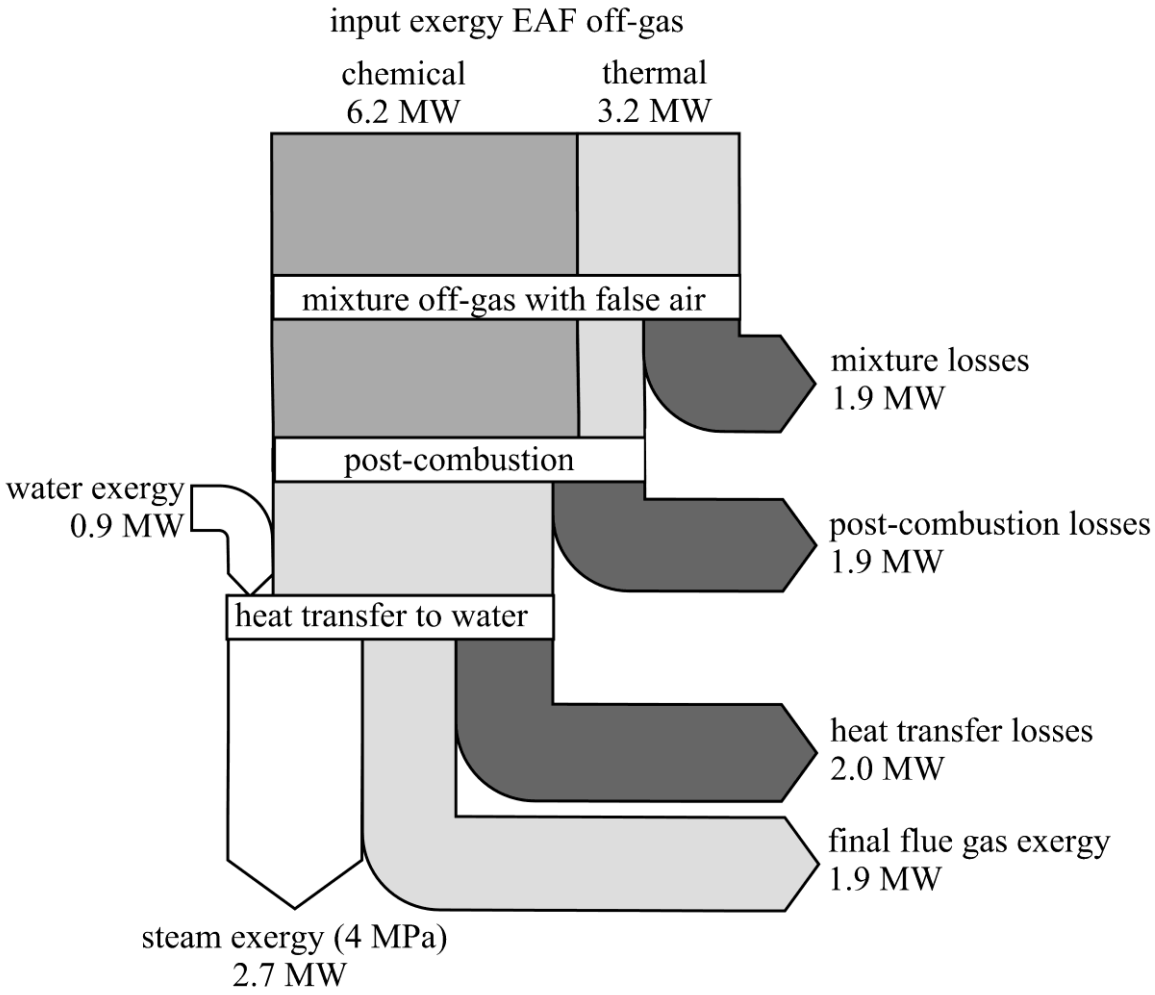

(b) Case of overstoichiometric combustion (II).

Fig. 3. Sankey diagrams.

Tables

Table 1. Technical parameters of EAFs within the EU.[7)]

technical parameter	value
tapping weight	100-160 t
primary + secondary exhaust gas flow	1-2*10^6 m^3_{STP} h^{-1}
number of charged baskets	1-3
tap-to-tap time	50-90 min

Table 2. Technical parameters of the sample EAF.[9)]

technical parameter	value
tapping weight	145 t
annual production	750,000 t per year
primary exhaust gas flow	120,000 m^3_{STP} h^{-1}
secondary exhaust gas flow	660,000 m^3_{STP} h^{-1}
number of charged baskets	3
tap-to-tap time	80 min
manufactured product	stainless steel

Table 3. Results concerning calculations the of steam coolant.

		pressure level [MPa]			
variable	unit	1	2	3	4
$m_{CS,tot,I}$ in t	[t_{CS} in min]	25.3 in 70	26.6 in 69	27.7 in 68	28.8 in 68
$m_{CS,tot,II}$ in t	[t_{CS} in min]	16.5 in 54	16.2 in 52	16.1 in 51	16.1 in 50
$\dot{B}_{W,I}$	[MW]	0.7	1.0	1.2	1.5
$\dot{B}_{W,II}$	[MW]	0.4	0.6	0.7	0.9
$\dot{B}_{transf,FG\text{-}CS,I}$	[MW]	3.6	3.5	3.5	3.4
$\dot{B}_{transf,FG\text{-}CS,II}$	[MW]	2.4	2.1	2.0	1.8
$\dot{B}_{CS,I}$	[MW]	4.3	4.5	4.7	4.9
$\dot{B}_{CS,II}$	[MW]	2.8	2.7	2.7	2.7
$B_{CS,tot,I}$	[GJ]	21	21	22	23
$B_{CS,tot,II}$	[GJ]	13	13	13	13
η_I	[-]	0.42	0.42	0.43	0.43
η_{II}	[-]	0.28	0.27	0.26	0.26